

Solar-Induced Stratospheric Circulation Changes

Gordana Jovanovic^{1,*}

¹Faculty of Science and Mathematics, University of Montenegro, Džordža Vasiingtona bb, 81000 Podgorica, Montenegro

Abstract. The propagation of gravity waves (GWs) and their reflection at the upper stratosphere-lower mesosphere discontinuity during maximum 11-year solar activity are studied. Solar activity is represented by a temperature increase of 2.5 K in the tropical upper stratosphere. A standard set of hydrodynamic (HD) equations, along with the dispersion relation and the equation for the reflection coefficient, is applied to the upper stratosphere-lower mesosphere discontinuity to determine which portions of the GW spectrum are most likely to propagate across it and influence the dynamics of the middle atmosphere. We find that the GW reflection increases noticeably during maximum 11-year solar activity. Gravity waves with $v_h < 31\text{ms}^{-1}$ are strongly attenuated at the upper stratosphere-lower mesosphere discontinuity, while waves with $31\text{ms}^{-1} < v_h < 279\text{ms}^{-1}$ are much more likely to enter the mesosphere. As a result, the GW flux reaching the lower mesosphere is reduced, thereby decreasing the ability of GWs to dissipate, transfer momentum to the mean flow, and drive the Brewer-Dobson Circulation (BDC). Since this is primarily a wave-driven circulation, the BDC is weaker during maximum solar activity than under normal stratospheric conditions. The connection between the lower mesosphere and BDC in the upper stratosphere is explained by the downward control principle.

1 Introduction

The 11-year solar cycle is presented by changes in the number of sunspots on the Sun's surface. The sunspots are darker because they are colder than the photosphere's background. They are surrounded by much brighter and therefore warmer faculae, Figs. 1, 2. On average, the brightening effect of faculae prevails, leading to variations of about 1 Wm^{-2} in the total solar irradiance (TSI) [1], primarily in the ultraviolet (UV) portion of the solar spectrum. Although the solar cycle affects the total solar irradiance (TSI) by only about 0.1%, variations in the ultraviolet (UV) region near 200 nm can reach up to 8% ([2], [3]). An increase in UV radiation can cause warming of up to 3 K in the tropical upper stratosphere ([4], [5]) and increase ozone concentration by approximately 2% ~ 5% over the complete 11-year solar cycle [6]. Namely, this enhancement in ozone concentration enhances the warming near the tropical upper stratosphere-lower mesosphere (~ 55 km) due to increased absorption by ozone of radiation with wavelengths between 240 and 320 nm ([7], [8]). The enhanced temperature gradient between low and high latitudes initiates a circulation pattern referred to as the Brewer-Dobson circulation (BDC) ([9], [10]). It is a large-scale stratospheric circulation

*e-mail: gordanaj@ucg.ac.me

in which air rises from the tropics, moves toward the poles, and then descends back into the troposphere. The BDC does not only depend on radiative forcing, i.e. on the temperature gradient, but is primarily a mechanically forced circulation, with the driving force provided by atmospheric planetary waves (PWs) and gravity waves (GWs). These waves propagate upwards from the troposphere into the middle atmosphere. As the density decreases with the altitude, the amplitude of these waves grows until they break at upper levels in the stratosphere/mesosphere. When breaking, these waves dissipate, transfer their momentum to the mean flow and drive the BDC circulation [11]. As the 11-year solar cycle modulates diabatic heating directly and also alters the background state encountered by upward propagating waves, it is reasonable to expect changes in the BDC. Solar maximum has been linked to a weakened BDC [12]. This weakening of the BDC is dynamically driven, and specifically is associated with reduced wave convergence in subpolar latitudes (approximately $50^{\circ} - 70^{\circ}$ latitude) in response to enhanced UV [9]. Also, Kodera and Kuroda [12] suggested that wind and temperature responses to the 11-year solar cycle in the polar stratosphere and mesosphere propagate downward and poleward by altering the propagation of PWs and GWs. According to the downward control principle proposed in Haynes et al. [13], wave disturbances are an agent transporting energy and momentum and affecting meridional circulation, so the study of meridional transport in all atmospheric layers directly concerns atmospheric waves—both PWs and GWs [14]. Core idea of downward control principle is that the wave drag (wave momentum deposition) at a given altitude controls the circulation at all levels below it. Changes in the conditions of atmospheric wave propagation and reflection during the increased solar activity in 11-year solar cycle are main mechanisms for transmitting the effect of the solar activity changes from the mesosphere to the underlying atmospheric levels. Garcia and Boville [15] stress that the winter mesospheric GW forcing can have effects down to ~ 30 km in the high latitude stratosphere.

This article focuses on propagation and reflection of GWs at the upper stratosphere-lower mesosphere during maximum solar activity. These waves are part of the acoustic-gravity wave spectra. We used the downward control principle to explain how the GW dissipation in the upper stratosphere-lower mesosphere drives the stratospheric circulation. Namely, GWs propagate upward and change the stratospheric circulation when their amplitude grow enough to break and be dissipated. Depending on the phase speed of the waves and the velocity of the background wind, one can define a critical layer where the intrinsic frequency¹ of the waves would approach the inertial frequency and the vertical wavelength would approach zero [16]. This occurs when the phase velocity of the GW is equal to the background wind speed. If such a critical layer is present, GWs will break somewhere below that level and deposit more momentum already in the stratosphere. We analysed the upward propagation of GWs through the Earth's atmosphere, modelled by two different temperature layers separated by a horizontal plane boundary. The analytical equation for the reflection coefficient is derived and applied to the upper stratosphere-lower mesosphere discontinuity during the increased solar activity.

Although GWs are an important element in understanding the responses of the atmospheric circulation to the solar cycle, there have only been a few observational studies that have investigated the impact of the solar cycle on GWs in the atmosphere using ground-based observations [17]. Furthermore, previous studies discussed the structure and strength of the BDC only in the lower stratosphere, and its structure in the middle and upper stratosphere has not yet been examined in detail [18].

¹Intrinsic frequency refers to the frequency of a wave as seen by the moving air (background flow), not by a stationary observer. It's essentially the relative frequency between the wave and the wind.

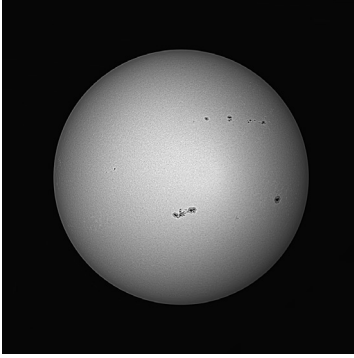


Figure 1. Solar photosphere with sunspots recorded on 27.5.2023. in Observatory Zeta, Goričani, Podgorica, Montenegro during the rising phase of the 25th solar cycle.

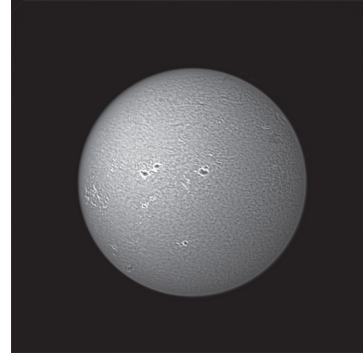


Figure 2. Solar chromosphere with sunspots and faculae recorded on 21.4.2025. in Observatory Zeta, Goričani, Podgorica, Montenegro during the maximum of the 25th solar cycle.

2 Theoretical background

The dispersion equation for GWs can be derived from the standard set of hydrodynamic equations that describe the dynamics of adiabatic processes in the neutral atmosphere stratified by gravity with constant acceleration (see details in [19] and [20]). These waves at the plane boundary between two regions are partially reflected. The reflection coefficient, defined as the square of the absolute value of the reflection amplitude, has been derived in previous papers [20], [21]. It depends on the temperature ratio between the two regions $s = T_1/T_2$, as well as on the horizontal (V_h) and vertical (V_{v1} and V_{v2}) phase velocities of the GWs:

$$R = \left[\frac{\left[\left(1 - \frac{\gamma}{2}\right) \left(\frac{1}{V_h^2 - 1} - \frac{s^2}{sV_h^2 - 1} \right) + \frac{(s-1)}{V_h^2} \right]^2 + \frac{\gamma^2 \Omega^2}{V_{v1}^2} \left(\frac{V_{v1}^2}{V_{v2}^2} \cdot \frac{s^2}{(sV_h^2 - 1)^2} - \frac{1}{(V_h^2 - 1)^2} \right)}{\left[\left(1 - \frac{\gamma}{2}\right) \left(\frac{1}{V_h^2 - 1} - \frac{s^2}{sV_h^2 - 1} \right) + \frac{(s-1)}{V_h^2} \right]^2 + \frac{\gamma^2 \Omega^2}{V_{v1}^2} \left[\frac{V_{v1}}{V_{v2}} \cdot \frac{s}{sV_h^2 - 1} + \frac{1}{V_h^2} \right]^2} \right]^2 + \left[\frac{\frac{2\gamma\Omega}{V_{v1}(V_h^2 - 1)} \left[\left(1 - \frac{\gamma}{2}\right) \left(\frac{1}{V_h^2 - 1} - \frac{s^2}{sV_h^2 - 1} \right) + \frac{(s-1)}{V_h^2} \right]}{\left[\left(1 - \frac{\gamma}{2}\right) \left(\frac{1}{V_h^2 - 1} - \frac{s^2}{sV_h^2 - 1} \right) + \frac{(s-1)}{V_h^2} \right]^2 + \frac{\gamma^2 \Omega^2}{V_{v1}^2} \left[\frac{V_{v1}}{V_{v2}} \cdot \frac{s}{sV_h^2 - 1} + \frac{1}{V_h^2} \right]^2} \right]^2. \quad (1)$$

Here, $\gamma = c_p/c_v = (j + 2)/j$ is the ratio of specific heats for a gas particle with $j = 5$ degrees of freedom, and $\Omega = \omega H/v_s$ is the dimensionless wave frequency, defined in terms of the frequency ω , the scale-height $H = v_s^2/\gamma g$, and the sound velocity v_s .

3 Results

In this article, we compare the reflection coefficient of GWs propagating from the stratosphere upward toward the mesosphere under normal stratospheric conditions and during periods of increased solar activity. Under normal stratospheric conditions, the temperature in the middle stratosphere (at approximately 35 km altitude) is $T_1 = 240$ K, $\gamma = 1.4$, sound velocity is $v_s = \sqrt{\gamma RT} = 310 \text{ms}^{-1}$, and the scale-height is $H=7000$ m. The Brunt-Väisälä frequency is $\omega_{BV} = \sqrt{\gamma - 1}g/v_s = 0.02 \text{s}^{-1}$. The temperature in the upper stratosphere-lower mesosphere (at approximately 55 km altitude) is $T_2 = 270$ K, ([22], [23]). Therefore, the parameter s

is given by $s = T_1/T_2 = 0.89$. It is known from the literature that GWs propagate in both regions—the stratosphere and the mesosphere if $\Omega < \sqrt{s}\Omega_{BV} = 0.42$, i.e. $\omega < 0.019s^{-1}$ and $V_h < 0.9$, [21]. Since $V_h = \Omega/K_p = v_h/v_s$, the horizontal phase velocity v_h depends on the sound velocity v_s in the atmospheric layer. Therefore, GWs propagating from the stratosphere to the mesosphere have a horizontal phase velocity of $v_h < 279ms^{-1}$.

The reflection coefficient of GWs propagating from the stratosphere to the mesosphere under normal stratospheric conditions is shown in Fig. 3. It increases with increasing frequency Ω and decreasing horizontal phase velocity V_h , [21]. Gravity waves with $\Omega < 0.2$ (i.e. $\omega < 0.009s^{-1}$) and $0.1 < V_h < 0.9$ (i.e. $31ms^{-1} < v_h < 279ms^{-1}$) are the most likely to enter the mesosphere, Fig. 3. During maximum solar activity, the temperature in the upper

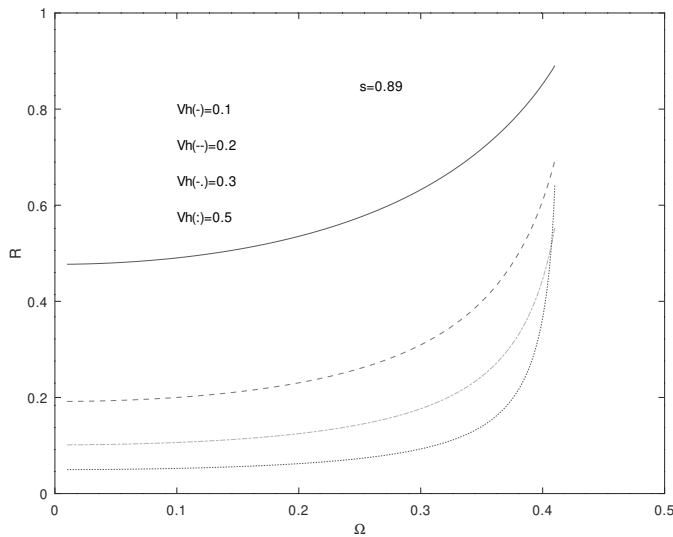


Figure 3. The reflection coefficient of gravity waves at the upper stratosphere-lower mesosphere discontinuity under normal stratospheric conditions, shown as a function of frequency, with horizontal phase velocity V_h and $s = T_1/T_2 = 0.89$ as parameters.

stratosphere-lower mesosphere can rise by up to 3K, [4]. For a temperature increase of 2.5 K, the temperature in this layer is $T_2 = 270 K + 2.5 K = 272.5 K$. Therefore, the parameter $s = T_1/T_2$ changed and becomes $s = 240K/272.5K = 0.88$. This alters the conditions for GW propagation. They can propagate in both the stratosphere and the mesosphere if $\Omega < \sqrt{0.88}\Omega_{BV} = 0.422$, i.e. with a slightly decreased frequency $\omega < 0.0187s^{-1}$. This 2.5 K temperature change leads to a noticeable increase in the reflection coefficient, as shown in Figs. 3 and 4. Consequently, GWs propagate less efficiently from the stratosphere to the mesosphere during periods of maximum solar activity compared to normal stratospheric conditions. If the phase velocity of these waves equals the wind speed in the upper stratosphere, the waves will reach a critical level. The waves then dissipate and deposit their momentum in the stratosphere. Koval et al. [24] found that solar activity affecting the meridional temperature gradient consequently changes the vertical structure of the zonal wind and propagation and reflection conditions for GWs. The latter is in agreement with the results presented here.

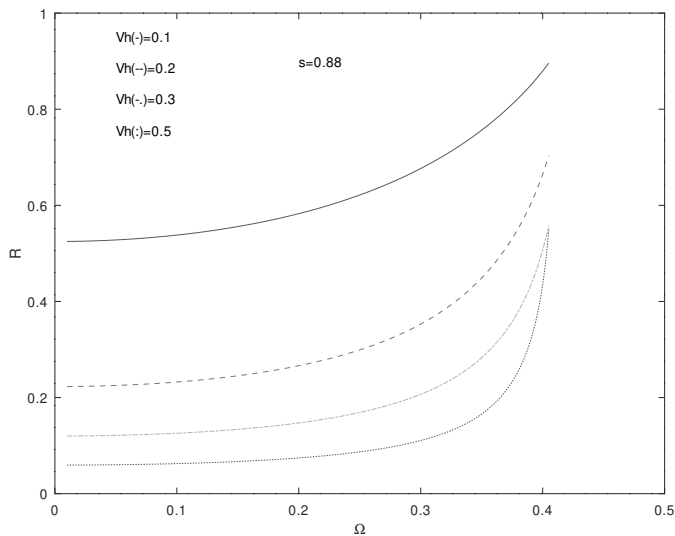


Figure 4. The reflection coefficient of gravity waves at the upper stratosphere-lower mesosphere discontinuity during maximum solar activity, shown as a function of frequency, with horizontal phase velocity V_h and $s = T_1/T_2 = 0.88$ as parameters.

4 Discussion

The vertical propagation of GWs is governed by the background temperature and wind in relation to their horizontal phase speed [25]. Dissipation (i.e. wave-induced momentum deposition) of GWs propagating upward at tropical latitudes provides the forcing that drives or helps to drive the stratospheric circulation [16]. The key mechanism is downward control. Gravity waves that dissipate at the upper stratosphere-lower mesosphere discontinuity drive the circulation in the stratosphere below. Downward control explicitly shows that this circulation is a compensating flow for wave dissipation ([11], [13], [24]). A comparison of Figs. 3 and 4 shows that the reflection coefficient increases during periods of maximum solar activity, and GWs propagate less efficiently from the stratosphere to the mesosphere. Therefore, the decrease in upward GW flux means potentially less wave-induced momentum deposition in the mesosphere and, consequently, driving force for the stratospheric BDC is weaker. This is in agreement with the statements in Givon et al. [9] and Kodera and Kuroda [12]. The weaker downward motion of the BDC produces less adiabatic warming in the high latitude region, leading to a cooler polar stratosphere [17]. Furthermore, changes in the BDC impact the global climate by altering tropopause properties, including static stability and the latitudes of the westerly jets ([18], [27]). Gan et al. [28] found that under solar maximum conditions, PW activity is weaker, resulting in a westerly zonal wind anomaly in the upper winter stratosphere and lower mesosphere. According to Gacia and Boville [15] this indicate that the downward influence of mesospheric GW breaking is most important where PW driving in the stratosphere is weak. Wang et al. [29] reported that stratospheric GW disturbances in high latitude regions are highly sensitive and respond rapidly to variations in solar activity. In contrast, in mid-latitude and equatorial regions, the response is delayed. The correlation increases gradually over this lag, reaching a very strong level after about two years.

Recent studies have shown that GWs break in the upper stratosphere-lower mesosphere and generate higher order gravity waves ([30], [31], [32]).

Cnossen et al. [4] demonstrate a distinct impact of how GW effects are represented on the downward and poleward propagation of an idealized solar forcing in the upper stratosphere. Differences between the gravity wave scheme and Rayleigh friction simulations occur in terms of the timing and extent of poleward and downward propagation of the responses in the stratosphere, and also, in general, in the responses in the troposphere.

5 Conclusion

Solar activity is the primary natural driver of temperature and ozone concentration variations in the stratosphere. It should be kept in mind that ozone is the most important absorber of solar UV radiation in the stratosphere, and even small differences in its distribution may influence the temperature field [33]. An increase in temperature in the tropical upper stratosphere strengthens the meridional temperature gradient between low and high latitudes, driving stratospheric circulation patterns such as the Brewer-Dobson Circulation (BDC). However, the BDC is essentially a mechanically forced circulation, driven by planetary waves (PWs) and gravity waves (GWs).

In this article, the characteristics of GWs during maximum solar activity are studied. Hydrodynamic (HD) equations and temperature, as the main parameters, are applied to the upper stratosphere-lower mesosphere discontinuity. A noticeable increase in the reflection coefficient is found during solar maximum. This implies that the flux of GWs entering the mesosphere is reduced, which decreases GW dissipation and the transfer of momentum to the mean flow in the mesosphere. The downward control principle is applied as the coupling mechanism between the mesosphere and stratospheric BDC circulation. This means that less wave dissipation in the mesosphere causes a weaker stratospheric BDC. Waves with the best chance to pass the upper stratosphere-lower mesosphere discontinuity and enter to the mesosphere are those with phase velocities $31\text{ms}^{-1} < v_h < 279\text{ms}^{-1}$.

Detailed studies of the interactions between mesospheric GWs and the mean circulation remain to be performed, and this will be the subject of future research. Another open question concerns other solar activity mechanisms beyond changes in UV radiation, such as solar magnetic field variations, which modulate the latitudinal distribution of the galactic cosmic ray (GCR) flux. GCR modulation alters atmospheric conductivity, thereby changing the conditions for the propagation of atmospheric waves and for circulation [33]. Variations in stratospheric circulation may, in turn, influence regional climate and weather patterns [34].

References

- [1] P. Foukal, C. Fröhlich, H. Spruit, T. Wigley, *Nature* (2006) <https://doi.org/10.1038/nature05072>
- [2] I. Ermolli et al., *Atmos Chem Phys*. (2013) <https://doi.org/10.5194/acp-13-3945-2013>
- [3] O. Coddington, J. Lean, P. Pilewskie, M. Snow, D. Lindholm, *Bull Amer Meteor Soc*. (2016) <https://doi.org/10.1175/BAMS-D-14-00265.1>
- [4] I. Cnossen, H. Lu, C.J. Bell, L.J. Gray, M.M. Joshi, *J. Geophys. Res.* (2011) doi:10.1029/2010JD014535
- [5] E.M. Bednarz, A.C. Maycock, P. Braesicke, P.J. Telford, N.L. Abraham, J.A. Pyle, *Atmos. Chem. Phys.* (2019) <https://doi.org/10.5194/acp-19-9833-2019>
- [6] N.F. Arnold, T.R. Robinson, *Ann. Geophys.* (1998) <https://doi.org/10.1007/s00585-997-0069-3>

- [7] J. D. Haigh, *Nature* (1994) <https://doi.org/10.1038/370544a0>
- [8] L.J. Gray et al., *Rev. Geophys.* (2010) doi:10.1029/2009RG000282
- [9] Y. Givon, C.I. Garfinkel, I. White, *J. Climate* (2021) <https://doi.org/10.1175/JCLI-D-20-0655.1>
- [10] K. Georgieva, S. Veretenenko, *Front. Astron. Space Sci.* (2023) doi: 10.3389/fspas.2023.1244402
- [11] N. Butchart, *Rev. Geophys.* (2014) <https://doi.org/10.1002/2013RG000448>
- [12] K. Kodera, Y. Kuroda, *J. Geophys. Res.* (2002) <https://doi.org/10.1029/2002JD002224>
- [13] P.H. Haynes, M.E. McIntyre, T.G. Shepherd, C.J. Marks, K.P. Shine, *J. Atmos. Sci.* (1991) DOI:10.1175/1520-0469(1991)048<0651:OTCOED>2.0.CO;2
- [14] A.V. Koval, N.M. Gavrilov, A.G. Golovko, K.A. Didenko, T.S. Ermakova, *Solar-terr. phys.* (2024) DOI: <https://doi.org/10.12737/stp-102202411>
- [15] R.R. Garcia, B. Boville, *J. Atmos. Sci.* (1994) doi:10.1175/1520-0469(1994)051<2238:COTMMC>2.0.CO;2
- [16] D.C. Fritts, M.J. Alexander, *Rev. Geophys.* (2003) <https://doi.org/10.1029/2001RG000106>
- [17] C.Y. Cullens, S.L. England R.R. Garcia, *J. Geophys. Res. Space Physics* (2016) doi:10.1002/2016JA022455
- [18] K. Sato, S. Hirano, *Atmos. Chem. Phys.* (2019) doi.org/10.5194/acp-19-4517-2019
- [19] B. Pinter, V.M. Čadež, B. Roberts, *Astron. Astrophys.* 346, 190?198 (1999)
- [20] G. Jovanovic, *Ann. Geophys.* (2024) <https://doi.org/10.5194/angeo-42-491-2024>
- [21] G. Jovanovic, *Atmos. Chem. Phys.* (2025) <https://doi.org/10.5194/acp-25-2979-2025>
- [22] X. Liu, J. Yue, J. Xu, L. Wang, W. Yuan, J.M. Russell III, M.E. Hervig, *J. Geophys. Res. Atmos.* (2014) doi:10.1002/2013JD021439
- [23] J.T. Emmert, D.P. Drob, J.M. Picone, D.E. Siskind, M.Jr. Jones, M.G. Mlynczak, et al., *Earth Space Sci.* (2020) <https://doi.org/10.1029/2020EA001321>
- [24] A.V. Koval, N.M. Gavrilov, A.I. Pogoreltsev, N.O. Shevchuk, *J. Atmos. Solar-Terr. Phys.* (2018) DOI: 10.1016/j.jastp.2018.03.012
- [25] P.K. Nyassor, C.M. Wrasse, I. Paulino, E. Yi?it, V.Y. Tsali-Brown, R.A. Buriti, C.A.O.B. Figueiredo, G.A. Giongo, F. Egito, O.M. Adebayo, H. Takahashi, D. Gobbi, *Atmos. Chem. Phys.* (2025) <https://doi.org/10.5194/acp-25-4053-2025>
- [26] M. Abalos, N. Calvo, S. Benito-Barca, H. Garny, S.C. Hardiman, P. Lin, M.B. Andrews, N. Butchart, R. Garcia, C. Orbe, D. Saint-Martin, S. Watanabe, K. Yoshida, *Atmos. Chem. Phys.* (2021) doi:10.5194/acp-21-13571-2021
- [27] J. Kidston, A.A. Scaife, S.C. Hardiman, D.M. Mitchell, N. Butchart, M.P. Baldwin, L.J. Gray, *Nat. Geosci.* (2015) <https://doi.org/10.1038/NGEO2424>
- [28] Q. Gan, J. Du, V.I. Fomichev, W.E. Ward, S.R. Beagley, S. Zhang, J. Yue, *J. Geophys. Res.: Space Physic* (2017) <https://doi.org/10.1002/2016JA023564>
- [29] C. Wang, Q. Mi, F. He, W. Guo, X. Zhang, J. Yang, *Remote Sens.* (2024) <https://doi.org/10.3390/rs16173239>
- [30] E. Becker, S.L. Vadas, *J. Geophys. Res. Atmos.* (2018) <https://doi.org/10.1002/2017jd027460>
- [31] S.L. Vadas, J. Zhao, X. Chu, E. Becker *J. Geophys. Res. Atmos.* (2018) <https://doi.org/10.1029/2017jd027970>
- [32] S.L. Vadas, E. Becker, *J. Geophys. Res. Space. Physics* (2019) <https://doi.org/10.1029/2019ja026694>

- [33] B.A. Tinsley, Bull. Amer. Meteor. Soc. (2023) <https://doi.org/10.1175/BAMS-D-23-0065.1>
- [34] J.D. Haigh, M. Blackburn, R. Day, J. Climate (2005) <https://doi.org/10.1175/JCLI3472.1>
- [35] Journal Author, Article title. Journal **Volume**, page numbers (year). <https://doi.org/Article-DOI-number>
- [36] Book Author, *Book title* (Publisher, place, year) page numbers